iScience

CellPress
OPEN ACCESS

Article

Tricalbins Are Required for Non-vesicular Ceramide Transport at ER-Golgi Contacts and Modulate Lipid Droplet Biogenesis

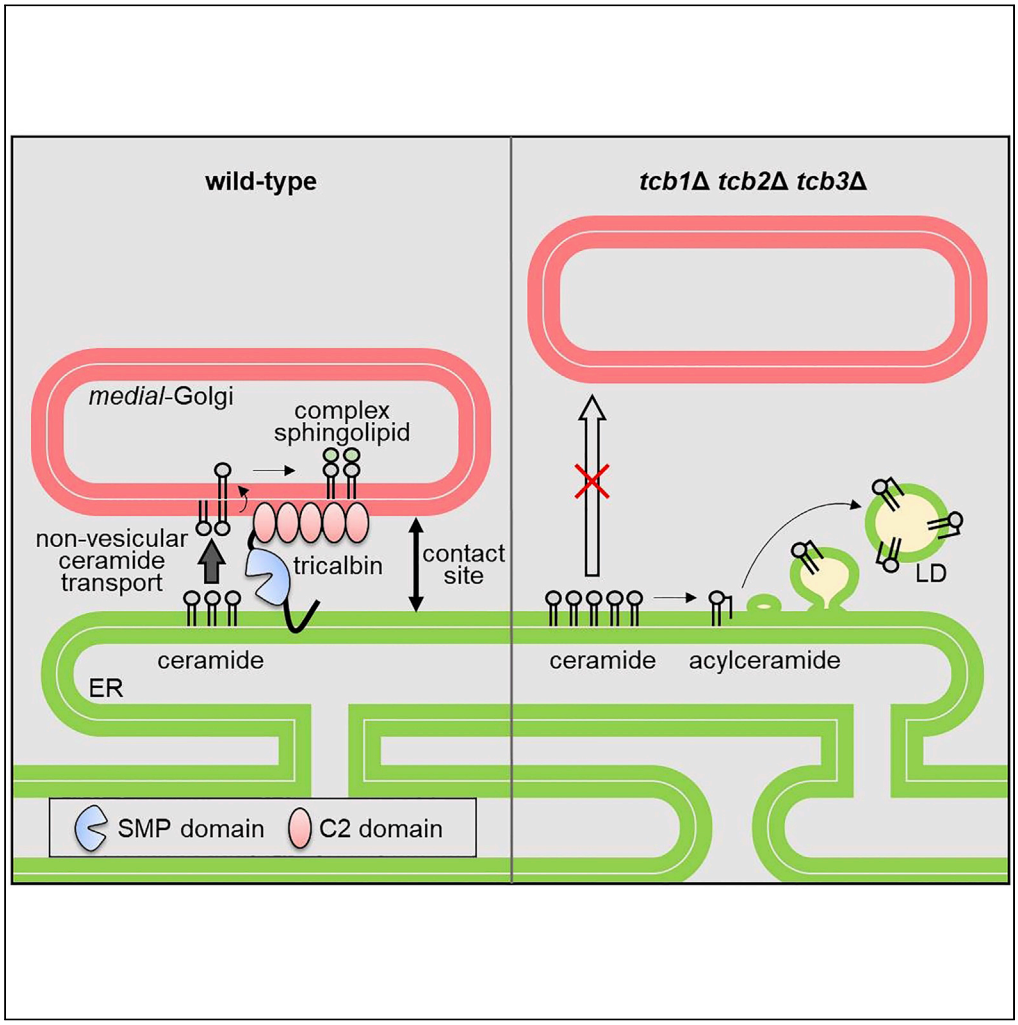

Atsuko Ikeda, Philipp Schlarmann, Kazuo Kurokawa, Akihiko Nakano, Howard Riezman, Kouichi Funato

kfunato@hiroshima-u.ac.jp

HIGHLIGHTS

Yeast tricalbin Tcb3p localizes at ER-Golgi contact sites

Lack of tricalbins reduces ER-Golgi contacts

Tricalbins regulate non-vesicular ceramide transport

Tricalbin deletion causes both acylceramide and lipid droplet accumulation

Ikeda et al., iScience 23, 101603
October 23, 2020
https://doi.org/10.1016/j.isci.2020.101603

iScience

CellPress
OPEN ACCESS

Article

Tricalbins Are Required for Non-vesicular Ceramide Transport at ER-Golgi Contacts and Modulate Lipid Droplet Biogenesis

Atsuko Ikeda,[1] Philipp Schlarmann,[1] Kazuo Kurokawa,[2] Akihiko Nakano,[2] Howard Riezman,[3] and Kouichi Funato[1,4,5,*]

SUMMARY

Lipid composition varies among organelles, and the distinct lipid composition is important for specific functions of each membrane. Lipid transport between organelles, which is critical for the maintenance of membrane lipid composition, occurs by either vesicular or non-vesicular mechanisms. In yeast, ceramide synthesized in the endoplasmic reticulum (ER) is transported to the Golgi apparatus where inositolphosphorylceramide (IPC) is formed. Here we show that a fraction of Tcb3p, a yeast tricalbin protein, localizes to ER-Golgi contact sites. Tcb3p and their homologs Tcb1p and Tcb2p are required for formation of ER-Golgi contacts and non-vesicular ceramide transport. Absence of Tcb1p, Tcb2p, and Tcb3p increases acylceramide synthesis and subsequent lipid droplet (LD) formation. As LD can sequester excess lipids, we propose that tricalbins act as regulators of ceramide transport at ER-Golgi contact sites to help reduce a potentially toxic accumulation of ceramides.

INTRODUCTION

Organelle membranes have unique lipid compositions, which relate to their physical properties, and specific function (Harayama and Riezman, 2018; van Meer et al., 2008). Membrane lipids are not only asymmetrically distributed in the leaflets of bilayers but also organized laterally into distinct domains (Sezgin et al., 2017; Simons and Ikonen, 1997). Such organization of membranes is achieved by transport and sorting of lipids from the endoplasmic reticulum (ER) to other organelles since the ER is the major site of lipid synthesis and the supplier of lipids to organelles (Holthuis and Levine, 2005; Holthuis and Menon, 2014; van Meer et al., 2008). Translocation of lipids across the bilayer and lateral segregation of lipids within a leaflet of membranes are also necessary for proper membrane organization (Holthuis and Levine, 2005; van Meer et al., 2008). Little is known, however, about the molecular mechanisms of lipid movement.

Ceramide is transported from the ER to the Golgi apparatus and incorporated into complex sphingolipids (Funato et al., 2002; Jain and Holthuis, 2017; Perry and Ridgway, 2005; Yamaji and Hanada, 2015). In mammalian cells, the ceramide transport protein (CERT) mediates non-vesicular trafficking of ceramide for sphingomyelin synthesis in the trans-Golgi (Hanada et al., 2003). The budding yeast *S. cerevisiae* uses both non-vesicular and vesicular ceramide transport pathways for inositolphosphorylceramide (IPC) synthesis (Funato and Riezman, 2001). *S. cerevisiae* has no CERT homolog, but a recent study reveals that Nvj2p promotes the non-vesicular transfer of ceramide from the ER to the Golgi (Liu et al., 2017). It was proposed that Nvj2p acts as a tether to establish membrane contact sites between the ER and the Golgi because Nvj2p is localized at ER-Golgi membrane contact sites and its overexpression increases ER-Golgi contact sites. ER-to-Golgi vesicular transport of ceramides in yeast is, on the other hand, mediated by COPII-coated vesicles (Funato and Riezman, 2001). This vesicular traffic accounts for 60%–80% of transport of ceramides (Kajiwara et al., 2014; Funato and Riezman, 2001). Previously, we showed that vesicular transport of ceramides is coupled with glycosylphosphatidylinositol (GPI) anchor biosynthesis and proposed that ceramides are transported to the Golgi by the same vesicles used for GPI anchored proteins (GPI-APs) (Kajiwara et al., 2008). In addition, we have shown that oxysterol-binding proteins regulate the vesicular transport of ceramides (Kajiwara et al., 2014).

Perturbation of ceramide transport or sphingolipid metabolism causes an accumulation of ceramides in the ER, leading to cellular dysfunction and death (Eisenberg and Büttner, 2014; Tani and Funato, 2018). One of

[1]Graduate School of Biosphere Science, Hiroshima University, Kagamiyama 1-4-4, Higashi-Hiroshima 739-8528, Japan

[2]Live Cell Super-Resolution Imaging Research Team, RIKEN Center for Advanced Photonics, 2-1 Hirosawa, Wako, Saitama 351-0198, Japan

[3]Swiss National Centre for Competence in Research in Chemical Biology and Department of Biochemistry, University of Geneva, 1211 Geneva, Switzerland

[4]Graduate School of Integrated Sciences for Life, Hiroshima University, Kagamiyama 1-4-4, Higashi-Hiroshima 739-8528, Japan

[5]Lead Contact

*Correspondence: kfunato@hiroshima-u.ac.jp

https://doi.org/10.1016/j.isci.2020.101603

the protection mechanisms preventing lipotoxicity when ceramide level is transiently increased appears to be to facilitate conversion of ceramides into complex sphingolipids. It is conceivable that degradation of ceramides by ceramidases also plays an important role to reduce the cellular level of ceramides (Ito et al., 2014; Kus et al., 2015; Voynova et al., 2015). In addition, experiments in mammalian cells showed that ceramides can also be converted to acylceramide and consequently incorporated into lipid droplets (LDs) to prevent the toxic accumulation of ceramides (Senkal et al., 2017); however, if a similar pathway exists in yeast has not been demonstrated, although it was proposed (Liu et al., 2017; Voynova et al., 2012).

In this study, we show that a conserved yeast ER membrane protein, tricalbin-3 (Tcb3p), localizes to contact sites between the ER and the Golgi. We also provide the first evidence to suggest that tricalbins are required for formation of ER-Golgi contact sites and non-vesicular transport of ceramides between the ER and Golgi compartments. In addition, we found that ceramide transport defects lead to increased acylceramide synthesis and subsequent LD formation, which may play a role in preventing the toxic accumulation of ceramides. Based on these results, we propose that yeast tricalbins regulate ER contacts with Golgi to mediate nonvesicular ceramide transport, which alleviates ceramide toxicity.

RESULTS

Overexpressed Tcb3-GFP Localizes to ER-Golgi Contact Sites and the Localization Requires the C2 Domains of Tcb3 and Other Tcb Proteins, Tcb1p, and Tcb2p

ER-plasma membrane (PM) tethering proteins, tricalbins (Tcb1p, Tcb2p and Tcb3p; yeast orthologs of the extended synaptotagmins, E-Syts), possess a transmembrane domain (TMD), a synaptotagmin-like mitochondrial lipid-binding protein (SMP) domain, and multiple C2 domains (Figure 1A) and localize to cortical ER (cER) (Kopec et al., 2010; Manford et al., 2012; Toulmay and Prinz, 2012). A recent study shows that Tcb3 protein level is upregulated in response to environmental changes, such as sterol depletion (Quon et al., 2018). To unravel the roles of tricalbins, we have re-examined the localization of Tcb3p. C-terminal tagged Tcb3-GFP was overexpressed under the control of the constitutive *TDH3* promoter and analyzed by fluorescent microscopy. As reported previously (Toulmay and Prinz, 2012), Tcb3-GFP expressed under the control of the endogenous *TCB3* promoter was localized in the cER but not in the perinuclear ER (nER) (Figure 1B), whereas overexpressed Tcb3-GFP was found in both cER and nER (Figure 1C). The TMD is essential for ER localization of Tcb3p because truncated forms of Tcb3p lacking the TMD (ΔTMD; SMP-C2 domains, ΔTMDΔC2; only SMP domain, ΔTMD-SMP; only C2 domains) are distributed in the cytosol or nucleus (see Figure S1). A truncated Tcb3(ΔSMP-C2)-GFP lacking the SMP and C2 domains localized to both the cER and nER (Figure 1D), but the nER/cER signal ratio of Tcb3(ΔSMP-C2)-GFP was higher than that of Tcb3-GFP (Figure 1E). In addition, Tcb3(ΔC2)-GFP lacking only C2 domains showed the same nER/cER ratio as Tcb3(ΔSMP-C2)-GFP, whereas no increase in the nER/cER ratio was seen with Tcb3(ΔSMP)-GFP lacking only SMP domain (Figure 1E). Thus, these results suggest that transmembrane and C2 domains but not SMP domain are required for localization of Tcb3p to the cER.

Remarkably, we found that overexpressed Tcb3-GFP localizes to dot-like structures on the ER (Figure 1C). The Tcb3-GFP puncta were decreased in strains expressing Tcb3 (ΔSMP-C2)-GFP and Tcb3(ΔC2)-GFP, although to a lesser extent, but not in strain expressing Tcb3(ΔSMP)-GFP (Figure 1F), indicating that the C2 domains of Tcb3p seem to be involved in the formation of Tcb3-GFP puncta. Tcb3-GFP puncta were preferentially localized in the nER (Figures 1C and 1G), and more importantly, they were found in close proximity to Golgi compartments (Figure 2A). Strikingly, they were enriched in regions in close proximity to the medial-Golgi compartments which contain Gos1p (Matsuura-Tokita et al., 2006; McNew et al., 1998). In parallel, close appositions between the cER and medial-Golgi were also found. Three-dimensional images reconstructed with two-dimensional confocal sections of Tcb3-GFP and mRFP-Gos1 fluorescence by the SCLIM system confirmed that medial-Golgi is located in the proximity of Tcb3p (Figure 2B). In addition, the time-lapse analysis revealed a dynamic behavior of ER-medial-Golgi contact sites (see Figure S2). Thus, these observations suggest that a portion of Tcb3p localizes to ER-Golgi contacts, and the C2 domains of Tcb3p play an important role in the localization of Tcb3p to ER-Golgi contact sites.

Tcb3p physically and functionally interacts with other Tcb proteins, Tcb1p and Tcb2p (Creutz et al., 2004; Tarassov et al., 2008). We asked whether Tcb1p and Tcb2p regulate Tcb3p localization. In cells lacking both Tcb1p and Tcb2p, the nER/cER signal ratio of Tcb3-GFP was unaffected as compared with the control cells (Figure 1H), but the number of cells with puncta (Figure 1I) was significantly reduced. These results suggest that Tcb1p and Tcb2p regulate the localization of Tcb3p to ER-Golgi contact sites but not to cER.

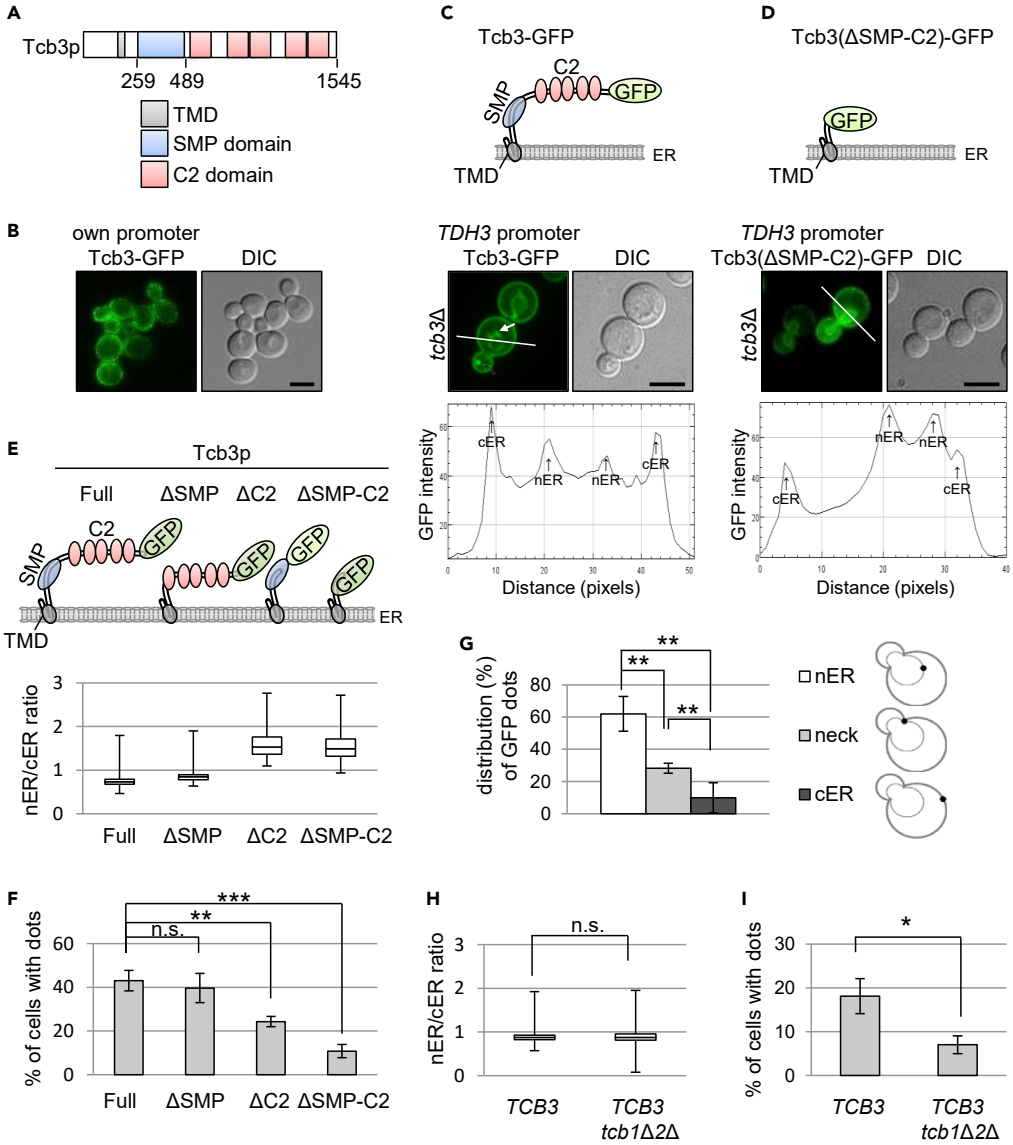

Figure 1. Overexpressed Tcb3-GFP Localizes to the Dot-like Domains of Perinuclear ER, and Its Localization Depends on C2 Domains and Tcb1p/Tcb2p

(A) Diagram of domain organization of Tcb3 protein. Amino acid length is indicated. TMD, transmembrane domain; SMP, synaptotagmin-like mitochondrial lipid-binding protein; C2, calcium-dependent lipid-binding domain.

(B) Endogenously expressed Tcb3-GFP localizes to cortical ER (cER) in wild-type cells. Cells expressing Tcb3p tagged with GFP at the C terminus under the control of *TCB3* endogenous promoter were grown at 25°C and imaged by differential interference contrast (DIC) and fluorescence microscopy. Scale bar, 5 μm.

(C–G) The C2 domains are required for Tcb3p localization to the dot-like domains of perinuclear ER (nER). *tcb3*Δ cells overexpressing Tcb3-GFP (C) or Tcb3(ΔSMP.C2)-GFP (D) under *TDH3* promoter were grown at 25°C and imaged by DIC and fluorescence microscopy. An arrow in the image in C indicates dot-like structures. Scale bar, 5 μm. Bottom panels are intensity plots along the white line in C and D. nER/cER intensity ratios for Tcb3-GFP, Tcb3(ΔSMP)-GFP, Tcb3(ΔC2)-GFP, and Tcb3(ΔSMP-C2)-GFP (E), percentages of cells with GFP dots (F) were quantified, and distribution of Tcb3-GFP dot was shown (G). The data represent the mean ± standard deviation (SD) of three independent experiments, each based on more than 100 cells. **$p < 0.01$ and ***$p < 0.001$ by Student's t-test. n.s., not significant.

(H and I) Tcb1p and Tcb2p are required for formation of Tcb3-GFP-positive dot structures. nER/cER intensity ratios for *tcb3*Δ and *tcb1*Δ *tcb2*Δ *tcb3*Δ cells expressing Tcb3-GFP under *TDH3* promoter (H) and quantification of percentages of cells with GFP dots (I). The data represent mean ± SD of three independent experiments, each based on more than 100 cells. *$p < 0.05$ by Student's t-test. n.s., not significant.

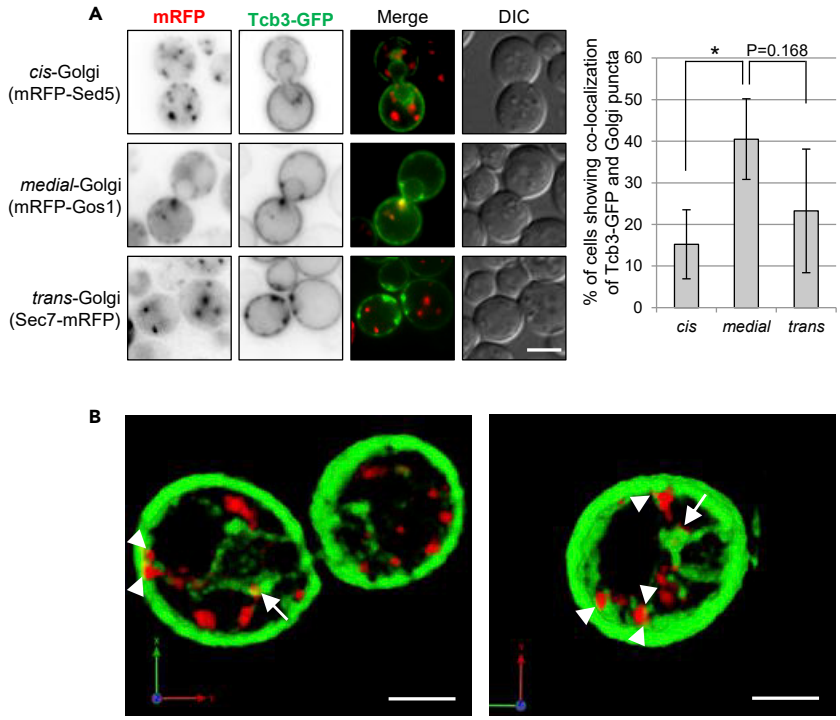

Figure 2. Overexpressed Tcb3-GFP Punctum Preferentially co-localizes with the Medial-Golgi-Resident Marker mRFP-Gos1

(A) *tcb3*Δ cells expressing Tcb3-GFP and mRFP-Sed5 (cis-Golgi marker) or mRFP-Gos1 (medial-Golgi marker) under *TDH3* promoter or Sec7-mRFP (trans-Golgi marker) under *ADH* promoter were grown at 25°C and imaged by DIC and fluorescence microscopy. The images were taken at 24 z-sections with 0.2-μm parallel intervals. Scale bar, 5 μm. The percentage of cells showing co-localization of Tcb3-GFP and mRFP-Sed5 puncta, mRFP-Gos1 puncta, or Sec7-mRFP puncta was quantified, and the data represent means ± SD of three independent experiments, each based on more than 60 cells. *$p < 0.05$ by Student's t-test.

(B) *tcb3*Δ cells expressing Tcb3-GFP with mRFP-Gos1 under *TDH3* promoter were observed with super-resolution confocal live imaging microscopy (SCLIM). Representative 3D images of whole cells are shown. Arrows in the images indicate nER-medial-Golgi contact sites, and arrowheads point to cER-medial-Golgi contact sites. Scale bar, 2 μm.

Elimination of Tcb Proteins Reduces ER-Golgi Contacts

As we found that a fraction of Tcb3p localized to ER-Golgi contact sites, this observation raised the possibility that Tcb proteins are required for formation of ER-Golgi contacts. To address this possibility, we assessed contacts between the ER and medial-Golgi by expressing the ER marker Kar2-SS-GFP and mRFP-Gos1. We quantified how often mRFP-Gos1 puncta were associated with the cER or nER. Although the total number of medial-Golgi vesicles containing mRFP-Gos1 in the cells was not affected by deletion of *TCB1*, *TCB2*, and *TCB3*, the number of medial-Golgi vesicles associated with the cER or the nER was significantly decreased in the *tcb1*Δ *tcb2*Δ *tcb3*Δ cells compared with wild-type control cells (Figure 3A). Similar results could be observed in cells lacking only Tcb3p (*tcb3*Δ cells) (Figure 3B). Tcb3(Full) and Tcb3(ΔSMP) were able to rescue the decrease of ER-Golgi contacts in *tcb3*Δ cells, whereas neither Tcb3 (ΔSMP-C2) nor Tcb3(ΔC2) restored them (Figure 3B). Collectively, these data suggest that Tcb proteins function as tethers to form ER-medial-Golgi contacts, and C2 domains are necessary to support the function of Tcb proteins.

Tcb Proteins Are Not Required for COPII-Mediated Vesicular Transport

Although to a limited great extent, Tcb3p was found in close proximity to cis-Golgi (Figure 2A). Since cis-Golgi contacts the ER exit sites (ERES) where COPII-coated buds are formed to mediate vesicular transport to the Golgi (Kurokawa et al., 2014), we tested whether Tcb proteins are needed for efficient vesicular transport of proteins from the ER. In *tcb1*Δ *tcb2*Δ *tcb3*Δ cells, neither the GPI-AP, Gas1p, nor the non-GPI-AP, carboxypeptidase Y (CPY), maturation was affected (see Figure S3A) at 24 or 37°C. As control, *sec18-20* mutant cells showed accumulation of immature proteins for both cargo proteins. Furthermore, a triple deletion of the *TCB* genes did not facilitate the accumulation of immature ER form of cargo proteins in

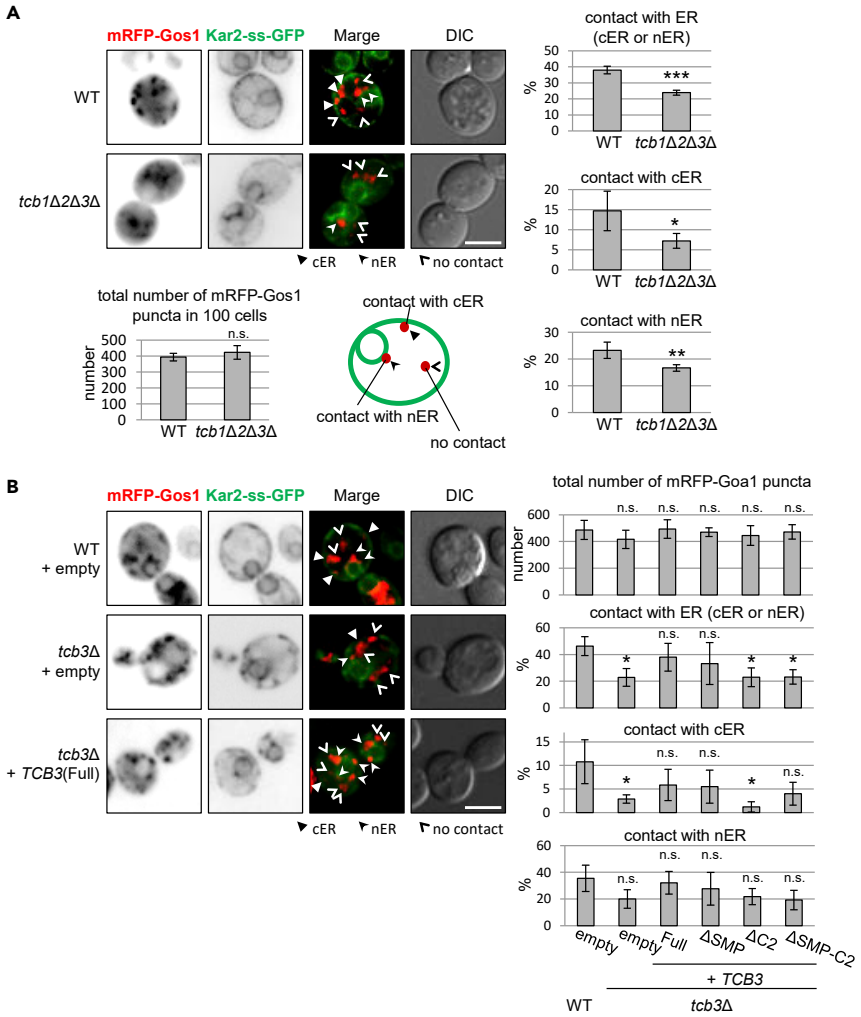

Figure 3. C2 Domains of Tcb3 Are Required to Form ER-medial-Golgi Contact

(A) Wild-type and *tcb1*Δ*2*Δ*3*Δ cells expressing mRFP-Gos1 (medial-Golgi marker) and Kar2-ss-GFP (ER marker) were grown at 25°C and imaged by DIC and fluorescence microscopy. Scale bar, 5 μm. The total number of mRFP-Gos1 puncta in 100 cells was quantified. The number of mRFP-Gos1 puncta associated with ER (cER or nER), cER, or nER was also quantified, and the results were expressed as percentage to the total number of mRFP-Gos1 puncta. Experiments were repeated three times; n = 300 cells. The data represent means ± SD of three experiments. *p < 0.05, **p < 0.01, and ***p < 0.005 by Student's t-test. n.s., not significant.

(B) *tcb3*Δ cells expressing mRFP-Gos1 (medial-Golgi marker) and Kar2-ss-GFP (ER marker) with empty, *TCB3*, *TCB3*(ΔSMP), *TCB3*(ΔC2), or *TCB3*(ΔSMP-C2) plasmid were grown at 25°C and imaged by DIC and fluorescence microscopy. Scale bar, 5 μm. The total number of mRFP-Gos1 puncta and the number of mRFP-Gos1 associated with the ER were quantified as described in (A), and the data represent means ± SD of three independent experiments. *p < 0.05 by Student's t-test. n.s., not significant.

sec18-20 mutant cells. These results suggest that Tcb proteins do not function as regulators of COPII vesicle-dependent transport from the ER. Consistent with this, we found no difference in numbers of puncta of Sec13-mCherry, which marks the ERES, between wild-type and mutant cells (see Figure S3B). In addition, we observed no co-localization of the overexpressed Tcb3-GFP with the puncta of Sec13-mCherry in *sec12-4* mutants under conditions that block COPII vesicle budding from the ER (see Figure S3C), which may also support the idea that Tcb proteins do not function in vesicular transport.

Tcb Proteins Are Required for Non-vesicular Ceramide Transport

The IPC synthase, Aur1p, is localized primarily in the medial-Golgi compartment (Levine et al., 2000). Therefore, this Golgi compartment is likely to be the site that receives and converts ceramides into

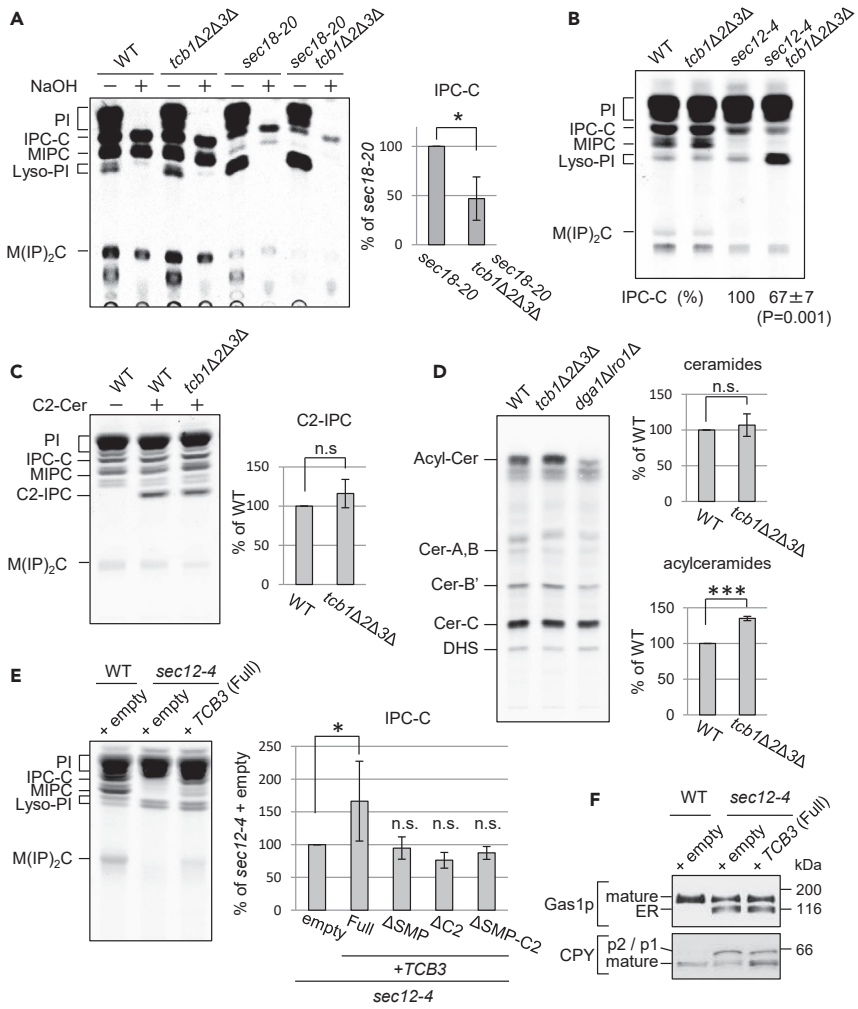

Figure 4. Tcb Proteins Are Required for Non-vesicular Ceramide Transport and Regulate Acylceramide Levels

(A and B) Cells were grown at 25°C, sifted to 37°C for 20 min (A) or 30°C for 30 min (B), and labeled with [^{3}H]*myo*-inositol for 1 h (A) or 1.5h (B). Labeled lipids were (+) or were not (−) mildly hydrolyzed with NaOH to deacylate glycerophospholipids and detect base-resistant complex sphingolipids (IPC-C, MIPC and M(IP)$_2$C) and applied to TLC plates using solvent system I. Incorporation (%) of [^{3}H]*myo*-inositol into IPC-C were quantified, and the percentage of the incorporation (%) in *sec18-20* (A) or *sec12-4* (B) was determined. Data represent mean ± SD of three independent experiments. *$p < 0.05$ by Student's t-test.

(C) Cells were grown at 25°C, incubated without (−) or with (+) C2-ceramide for 20 min, and labeled with [^{3}H]*myo*-inositol for 3 h. Labeled lipids were applied to TLC plates using solvent system I. Incorporation (%) of [^{3}H]*myo*-inositol into C2-IPC was quantified, and the percentage of the incorporation (%) in wild-type cells was determined. Data represent mean ± SD of three independent experiments. n.s., not significant by Student's t-test.

(D) Cells were grown at 25°C and labeled with [^{3}H]DHS for 3h. Labeled lipids were applied to TLC plates using solvent system II. Fractions containing ceramides and acylceramides on the TLC plate were collected by scraping and eluting the lipid extracts from the silica and analyzed by TLC using solvent system III. Incorporation of [^{3}H]DHS into ceramides (Cer-A, B, B′ and (C) or acylceramides was quantified, and the percentage of the total radioactivity (%) in wild-type cells was determined. Data represent mean ± SD of three independent experiments. ***$p < 0.001$ by Student's t-test. n.s., not significant.

(E) *sec12-4* cells transformed with empty, *TCB3*, *TCB3*(ΔSMP), *TCB3*(ΔC2), or *TCB3*(ΔSMP-C2) plasmid were grown at 25°C, sifted to 30°C for 30 min, and labeled with [^{3}H]*myo*-inositol for 1.5 h and chased for 2 h. Labeled lipids were applied to TLC plates using solvent system I, and the percentage of incorporation (%) of IPC-C in cells transformed with empty plasmid was determined. Data represent mean ± SD of three independent experiments. *$p < 0.05$ by Student's t-test. n.s., not significant.

Figure 4. *Continued*
(A–E) PI, phosphatidylinositol; IPC-C, inositolphosphorylceramide subclasses C; MIPC, Mannosyl inositolphosphorylceramide; Lyso-PI, lysophosphatidylinositol; $M(IP)_2C$, mannosyl di(inositolphosphoryl) ceramide.
(F) Wild-type and the same strains as in (E) were grown at 25°C and sifted to 30°C for 4 h. Cell lysates were prepared and subjected to SDS-PAGE, followed by Western blot analysis.

IPC. Although it is still unknown whether ceramide transfer to the Golgi occurs at ER-medial-Golgi contact sites, an *in vitro* assay revealed that non-vesicular transport of ceramides requires organelle contact (Funato and Riezman, 2001). Given that Tcb proteins participate in ER-medial-Golgi contact sites, we examined whether they are required for IPC synthesis. As shown in Figures 4A and 4B, IPC synthesis was severely reduced in *sec18-20* or *sec12-4* mutant cells at non-permissive temperatures, but was unaffected in *tcb1*Δ *tcb2*Δ *tcb3*Δ cells, suggesting that Tcb proteins are dispensable for vesicular transport of ceramides. This is consistent with the results showing normal transport of proteins (see Figure S3A). If Tcb proteins are required for non-vesicular ceramide transport, deletion of *TCB* genes combined with ER-to-Golgi *sec* mutations could lead to an additional reduction in IPC synthesis, greater than that in *sec*-mutant cells. Thus, we examined the effect of *TCB* gene disruption on IPC synthesis under conditions that block ER-to-Golgi vesicular trafficking of ceramides by *sec* mutations. When cells were labeled with [^{3}H]*myo*-inositol, we found that IPC synthesis was approximately 50% lower in *sec18-20 tcb1*Δ *tcb2*Δ *tcb3*Δ mutant cells than in *sec18-20* mutant cells (Figure 4A). Similar results were obtained with *sec12-4* mutants (Figure 4B). Together, these findings support a role for Tcb proteins in non-vesicular transport of ceramides but not in vesicular transport.

To exclude the possibility that deletion of *TCB* genes affects IPC synthesis activity, we analyzed the IPC synthesis activity in the *tcb1*Δ *tcb2*Δ *tcb3*Δ cells *in vivo* as described previously (Kajiwara et al., 2008). For this purpose, we used C2-ceramide that reaches the Golgi through a diffusion-mediated or an endocytic route when added exogenously to cells and measured the incorporation of exogenous C2-ceramide into C2-IPC. In comparison to wild-type cells, the incorporation of C2-ceramide into C2-IPC was not affected in *tcb1*Δ *tcb2*Δ *tcb3*Δ cells (Figure 4C). Similar results were obtained with *sec* background strains (the relative incorporation into C2-IPC [%] of *sec12-4 tcb1*Δ *tcb2*Δ *tcb3*Δ to *sec12-4* cells was 108%). Phosphatidylinositol (PI) is the substrate for the IPC synthesis enzyme converting C2-ceramide to C2-IPC. If Tcb proteins are involved in the delivery of PI to the site of IPC synthesis, *TCB* deletion should result in decreased C2-IPC synthesis. This was not the case. In addition, we measured the levels of ceramides in wild-type and *tcb1*Δ *tcb2*Δ *tcb3*Δ cells. The total ceramide levels were not decreased in the *tcb* mutant cells (Figure 4D). These results suggest that the IPC synthesis defect of the *tcb* mutant combined with the *sec* mutation is not due to reduced enzyme activity, impaired delivery of substrate PI, or a ceramide synthesis defect. Thus, we conclude that the problem is in delivery of the ceramide to the IPC synthesis enzyme and thus that Tcb proteins are required for non-vesicular ceramide transport.

We also investigated whether Tcb3p overexpression restores the IPC synthesis defect in *sec12-4* mutant cells. As shown in Figure 4E, overexpression of *TCB3* in *sec12-4* cells partially rescued the IPC synthesis defect. Because overexpression of *TCB3* did not suppress the protein transport defects of *sec12-4* mutant cells (Figure 4F), it is most likely that the restoration of IPC synthesis by *TCB3* overexpression results from stimulation of non-vesicular ceramide transport but not vesicular traffic. In addition, our data revealed that overexpression of mutants lacking the SMP domain, C2 domains, or SMP-C2 domains failed to rescue the IPC synthesis defect in *sec12-4* mutant cells (Figure 4E). Collectively, these results suggest that Tcb proteins are involved in non-vesicular ceramide transport and that both SMP and C2 domains of Tcb3p are required to transport ceramide efficiently at ER-Golgi contact sites.

The *tcb* mutant combined with the *sec* mutation caused increased levels in lysophosphatidylinositol (lyso-PI) (Figure 4B). Elevated levels of lyso-PI have been often observed in *sec* mutants such as *sec12*, *sec13*, *sec16*, *sec23*, *sec18*, *sec6*, *sec7*, and *sec14* at restricted temperatures (Figure 4A) (Puoti et al., 1991), suggesting that increase in the lyso-PI level is not specific for *TCB* deletion and vesicular transport processes may be involved in lyso-PI metabolism. As lysophospholipids facilitate COPII vesicle formation (Melero et al., 2018), the increased level of lyso-PI may function to attenuate the secretion defects of *sec* mutants in a feedback loop. Another possibility is that tricalbin-mediated ER-Golgi contact sites regulate transport of lyso-PI between the ER and other organelles including the Golgi and the PM or lyso-PI metabolism.

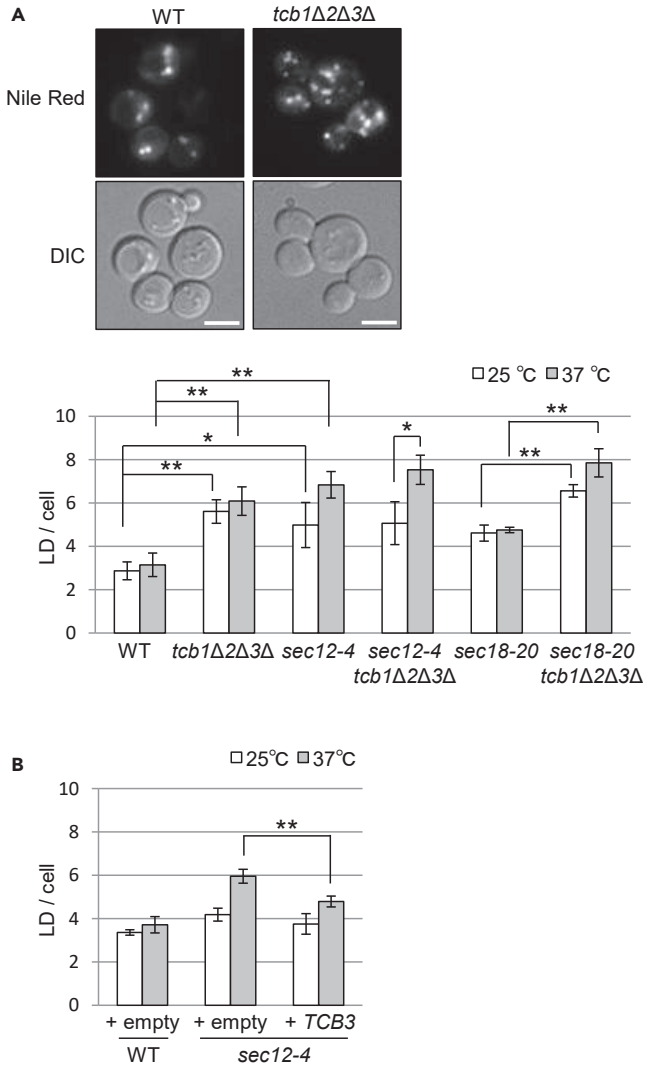

Figure 5. Inhibition of Ceramide Transport Facilitates LD Formation

(A and B) The same strains as in Figures 4A and 4B (A) and 4E (B) were grown at 25°C and then incubated at 25°C or 37°C for 30 min. Lipid droplets (LDs) were stained with Nile Red and imaged by fluorescence microscopy, and numbers of LDs per cell were counted. The data represent mean ± SD of three independent experiments, each based on more than 100 cells. *p < 0.05 and **p < 0.01 by Student's t-test.

Reduced Ceramide Transport Facilitates LD Formation

Overproduced lipids are converted to neutral forms and sequestered in LDs to alleviate lipotoxicity, resulting in an accumulation of LD (Walther and Farese, 2012). Ceramide is metabolized to acylceramide by acyltransferases Lro1p and Dga1p in *S. cerevisiae* (Voynova et al., 2012). This has been proposed to be a mechanism for removing excess ceramides from the ER (Liu et al., 2017; Tani and Funato, 2018; Senkal et al., 2017; Voynova et al., 2012). Given that we found that *tcb1*Δ *tcb2*Δ *tcb3*Δ cells accumulated acylceramide (Figure 4D), we explored the possibility that deletion of Tcb proteins or defect of vesicular transport leads to stimulation of LD formation. Cells were stained with Nile Red, a lipophilic dye to visualize LDs (Greenspan et al., 1985; Radulovic et al., 2013), and the number of LDs per cell was quantified. We found that LD formation was increased in *sec12-4* or *sec18-20* cells (Figure 5A). Lack of Tcb proteins also caused an enhanced LD formation. In addition, the coupling of *TCB* deletion and *sec18* mutation showed a maximal formation of LDs at a non-permissive temperature. These observations suggest that inhibition of ceramide transport or other potential substrates of Tcb proteins facilitates LD formation.

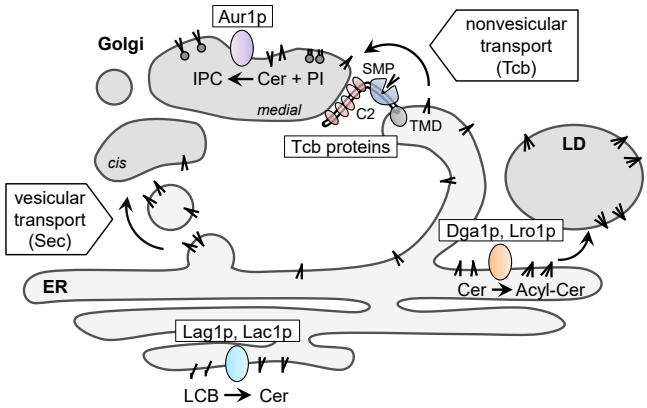

Figure 6. A Model for the Role of Tcb Proteins in Non-vesicular Ceramide Transport and LD Formation

Tcb proteins are required for non-vesicular transport of ceramide at ER-medial-Golgi contact sites. The SMP domains in Tcb proteins may transfer ceramide, and the C2 domains may tether the ER to the medial-Golgi via the interaction with acidic phospholipids. Ceramide transport defects result in ceramide accumulation, which may increase acylceramide formation, thereby facilitating LD formation to alleviate cells from ceramide toxicity.

Next, we tested if Tcb3p overexpression reduces LD formation in *sec12-4* mutant cells because it partially rescued the IPC synthesis defect in mutant cells (Figure 4E). As shown in Figure 5B, the increased LD formation at a non-permissive temperature in *sec12-4* mutant cells was rescued by overexpression of Tcb3p. Thus, these findings indicate that Tcb3p regulates LD formation negatively, consistent with the role of Tcb proteins in non-vesicular ceramide transport. These data also suggest that non-vesicular ceramide transport can alleviate abnormal LD formation caused by defects in vesicular transport. Collectively, these results support the idea that ceramide transport is critical for the regulation of ER ceramide levels and that LDs play an important role to alleviate toxicity caused by accumulation of excess ceramides in the ER, through formation of acylceramide.

DISCUSSION

Although Tcb proteins were initially identified as tethers localized at ER-PM contact sites and involved in regulation of PI4P metabolism (Manford et al., 2012; Toulmay and Prinz, 2012), our results revealed that a fraction of Tcb3p is also localized at contact sites with Golgi compartments and that Tcb3p and other Tcb proteins, Tcb1p and Tcb2p, play an important role in ER-Golgi contact formation (Figure 6). We also provide evidence to suggest roles of Tcb proteins in facilitating non-vesicular ceramide transport and in downregulating LD formation.

How might Tcb proteins promote non-vesicular ceramide transport? The SMP domains of Tcb proteins are required to localize proteins containing them to ER-PM contact sites and bind membranes (Toulmay and Prinz, 2012), suggesting that they may function to form membrane contacts. However, lack of the SMP domain in Tcb3p did not impact the number of ER-medial-Golgi contacts (Figure 3B). Because the mutant lacking the SMP domain still failed to synthesize IPC (Figure 4E), it is possible that the SMP domain mediates ceramide exchange between the ER and the Golgi. The SMP domains in the extended synaptotagmin-like proteins, E-Syts, which are mammalian orthologs of Tcb proteins, can bind and transfer lipids between membranes (Schauder et al., 2014; Yu et al., 2016). A large-scale protein-lipid interaction study using nitrocellulose arrays with immobilized lipids implied that Tcb3p binds phytoceramide (Gallego et al., 2010). Hence, the SMP domains in Tcb proteins may transfer ceramide. Alternatively, the SMP domains in Tcb proteins could function in concert with other lipid transfer proteins. As Nvj2 is localized at ER-Golgi contact sites (Liu et al., 2017) and an unknown cytosolic protein is required for non-vesicular ceramide transport (Funato and Riezman, 2001), they are possible candidates with the ability to bind and extract ceramides from the ER and deliver it to the Golgi.

In addition, our results suggest that the C2 domains of Tcb proteins are used to tether the ER to the Golgi because lack of the C2 domains in Tcb3p led to a decreased number of ER-medial-Golgi contact (Figure 3B). This is consistent with a study in mammalian cells, where knockdown of three E-Syts reduces

ER-PM contact sites in a cytosolic Ca^{2+}-regulated way, probably mediated by Ca^{2+}-binding C2 domains (Giordano et al., 2013; Min et al., 2007). As C2 domains of Tcb proteins bind acidic phospholipids, including phosphatidylserine and phosphoinositides (Gallego et al., 2010; Schulz and Creutz, 2004), ER-Golgi contacts could take place via the interaction of acidic phospholipids with C2 domains. Thus, we propose that Tcb proteins function as tethers or lipid transfer proteins at ER-Golgi contact sites to drive non-vesicular ceramide transport (Figure 6).

Given that Tcb3p puncta are found in close appositions with the medial-Golgi where the IPC synthase enzyme Aur1p is localized (Levine et al., 2000) and that Tcb3p appears to form a complex with Tcb1p and Tcb2p (Creutz et al., 2004; Tarassov et al., 2008), it is conceivable that Tcb protein complex acts as a functional tethering complex to form ER-medial-Golgi contacts, which can transfer ceramides directly to the medial-Golgi to efficiently feed into IPC synthesis. This is consistent with our data, which showed that Tcb1p and Tcb2p are required for formation of Tcb3p puncta, suggesting that they might be important for Tcb3p function. Interestingly, there was a synthetic effect of SMP deletion to C2 deletion on Tcb3p puncta formation (Figure 1F). As no such effect was observed for ER-Golgi contact formation (Figure 3B), SMP domain may be implicated in protein oligomerization to form stable Tcb protein complexes.

Because endogenous Tcb3p is selectively enriched in the cER even though a small part is localized to small dot-like structures on the nER (see Figure S4A), we wondered what conditions increase the nER localization and cause dot formation of Tcb3p. Nvj2p was shown to become enriched at ER-Golgi contacts when cells were treated with dithiothreitol (DTT), which causes ER stress (Liu et al., 2017). We found that ER stress by treatment with DTT or tunicamycin resulted in an increased number of cells with Tcb3-GFP dots (see Figures S4A and S4B), although the fluorescence intensity (or size) of the Tcb3-GFP dots is much lower than that of Tcb3-GFP dots when overexpressed. Some of the dots co-localize with mRFP-Gos1 (see Figures S4C and S4D). These findings suggest that endogenously expressed Tcb3-GFP becomes enriched at ER-Golgi contacts in response to ER stress. This is also consistent with the model that tricalbins play a role in preventing the accumulation of toxic lipids such as ceramide, which causes ER stress. It is noteworthy that tunicamycin treatment appears to impair the transport of ceramides between the ER and the Golgi (Pittet et al., 2006; Yabuki et al., 2019).

In addition to localization to nER-medial-Golgi contact sites, Tcb3p also localizes to contact sites between the cER and medial-Golgi. Thus, it is possible that ceramide transfer occurs at cER-medial-Golgi contact sites. Further work will be needed to determine the exact site where non-vesicular ceramide transport occurs.

How the impaired transport of ceramide facilitates LD formation is not fully understood, but we propose a model in which abnormal accumulation of ceramides in the ER caused by impaired ceramide transport leads to an elevated acylceramide level through activity of ER-localized Lro1p and Dga1p (Voynova et al., 2012), thereby stimulating LD formation. Indeed, a significant increase of acylceramide levels was observed in the *tcb1*Δ *tcb2*Δ *tcb3*Δ cells compared to wild-type cells (Figure 4D). Similar results were obtained with *sec* background strains (the relative acylceramide level [%] of *sec12-4 tcb1*Δ *tcb2*Δ *tcb3*Δ to *sec12-4* cells was 122%). The levels of triacylglycerides and sterol esters, which are the main components of the lipid droplet core structure, were significantly increased in *sec* mutants at non-permissive temperatures, but not in the cells lacking all three Tcb proteins (see Figures S5A and S5B); rather, the lack of Tcb proteins led to a reduced level of sterol esters, which might be due to a defect in retrograde transport of sterol from the PM to the ER (Quon et al., 2018). Therefore, these results imply that the enhanced LD formation in *tcb1*Δ *tcb2*Δ *tcb3*Δ cells results from the acylceramide accumulation caused by defect of non-vesicular ceramide transport. We have previously shown that LD formation is facilitated in *S. cerevisiae* mutant strains defective in GPI anchor synthesis and in GPI anchoring (Kajiwara et al., 2008). Mutant cells of the *S. pombe* gene homolog of *S. cerevisiae CWH43* gene, which is implicated in remodeling of GPI lipid moiety to ceramide (Ghugtyal et al., 2007; Umemura et al., 2007), were also shown to have increased numbers of LDs (Nakazawa et al., 2018). Since these *gpi* mutants cause IPC synthesis defects (Kajiwara et al., 2008), it is plausible that enhanced LD formation in these mutants results from increased ceramide levels through defects in vesicular transport of ceramides. Moreover, it is noteworthy that overexpression of *TCB3* suppressed the enhanced LD formation in *sec12-4* mutant cells. Because their overexpression did not affect vesicular protein traffic in the mutant cells, ceramides accumulated in the ER due to vesicular transport defects can likely be bypassed by non-vesicular transport routes. Thus, non-vesicular ceramide transport may

play important roles as a defense system to protect cells against the toxic accumulation of ceramide when vesicular traffic is impaired.

In summary, our studies suggest a new function for Tcb proteins in non-vesicular transport of ceramides at ER-Golgi contact sites. Further work is required to elucidate what features of medial-Golgi are recognized by the C2 domains of Tcb proteins, whether the SMP domain transfers ceramides between membranes, to identify the ligand-binding sites within the C2 domains and the SMP domain by biochemical methods using various point mutants and radioactive or photocrosslinkable ligands (Dadsena et al., 2019). Nvj2p has been shown to be an ER-Golgi tethering protein that facilitates the non-vesicular transfer of ceramides to the Golgi complex (Liu et al., 2017). It is an intriguing question whether tricalbins and Nvj2p have cooperative roles in ceramide transport. Also, a cytosolic protein(s) involved in non-vesicular ceramide transport (Funato and Riezman, 2001) still remains to be identified.

Limitation of the Study

Although our study reveals that tricalbins are involved in non-vesicular ceramide transport from the ER to the Golgi, it is unknown whether tricalbins have the ability to bind and extract ceramides from the ER and deliver it to the Golgi. One possibility is that SMP domain of Tcb3p may transfer ceramides. However, we could not show direct binding of SMP domain of Tcb3p to ceramides. Further studies will be required to determine whether tricalbins directly bind to ceramide or to identify other ceramide transfer proteins that may function in concert with tricalbins at ER-Golgi contact sites. We also wish to emphasize that nanometer distances between membranes at membrane contact sites are below the diffraction limit for light microscope. As electron microscopy, especially when correlated with light microscopy, is a powerful technique to analyze ultrastructure which cannot otherwise be seen, it might provide further insight into the role of tricalbins at ER-Golgi contact sites.

Resource Availability

Lead Contact

Further information and requests for resources should be directed to and will be fulfilled by the Lead Contact, Kouichi Funato (kfunato@hiroshima-u.ac.).

Materials Availability

Yeast strains and plasmids generated in this study will be made available on reasonable requests.

Data and Code Availability

The data that support the findings of this study are included in the article and its Supplemental Information, or are available from the corresponding authors on request.

METHODS

All methods can be found in the accompanying Transparent Methods supplemental file.

SUPPLEMENTAL INFORMATION

Supplemental Information can be found online at https://doi.org/10.1016/j.isci.2020.101603.

ACKNOWLEDGMENTS

We are grateful to Dr. R. Schekman for providing yeast *sec* mutant strains. This work was supported by the Japan Society for the Promotion of Science (JSPS), Grant-in-Aid for Scientific Research (KAKENHI), Japan [JP16K07693 and 19H02922 to K.F.], [JP25221103, JP16HD05419, JP17H06420 and JP18H05275 to K.K.], by a JSPS Research Fellowship for Young Scientists, Japan [18J10104 to A.I.], by the Swiss National Science Foundation, Switzerland [310030B_166686 to H.R,], and by the NCCR Chemical Biology funded by the Swiss National Science Foundation, Switzerland [51NF40-160589 to H.R.].

AUTHOR CONTRIBUTIONS

A.I. and K.F. designed the experiments. A.I., P.S., and K.K. performed the experiments. A.I., P.S., K.K., A.N., H.R, and K.F. analyzed data and wrote the manuscript.

DECLARATION OF INTERESTS

The authors declare no competing interests.

Received: April 20, 2020
Revised: July 20, 2020
Accepted: September 21, 2020
Published: October 23, 2020

REFERENCES

Creutz, C.E., Snyder, S.L., and Schulz, T.A. (2004). Characterization of the yeast tricalbins: membrane-bound multi-C2-domain proteins that form complexes involved in membrane trafficking. Cell Mol. Life Sci. *61*, 1208–1220.

Dadsena, S., Bockelmann, S., Mina, J.G.M., Hassan, D.G., Korneev, S., Razzera, G., Jahn, H., Niekamp, P., Müller, D., Schneider, M., et al. (2019). Ceramides bind VDAC2 to trigger mitochondrial apoptosis. Nat. Commun. *10*, 1832.

Eisenberg, T., and Büttner, S. (2014). Lipids and cell death in yeast. FEMS Yeast Res. *14*, 179–197.

Funato, K., and Riezman, H. (2001). Vesicular and nonvesicular transport of ceramide from ER to the Golgi apparatus in yeast. J. Cell Biol. *155*, 949–959.

Funato, K., Vallée, B., and Riezman, H. (2002). Biosynthesis and trafficking of sphingolipids in the yeast *Saccharomyces cerevisiae*. Biochemistry *41*, 15105–15114.

Gallego, O., Betts, M.J., Gvozdenovic-Jeremic, J., Maeda, K., Matetzki, C., Aguilar-Gurrieri, C., Beltran-Alvarez, P., Bonn, S., Fernández-Tornero, C., Jensen, L.J., et al. (2010). A systematic screen for protein-lipid interactions in *Saccharomyces cerevisiae*. Mol. Syst. Biol. *6*, 430.

Ghugtyal, V., Vionnet, C., Roubaty, C., and Conzelmann, A. (2007). *CWH43* is required for the introduction of ceramides into GPI anchors in *Saccharomyces cerevisiae*. Mol. Microbiol. *65*, 1493–1502.

Giordano, F., Saheki, Y., Idevall-Hagren, O., Colombo, S.F., Pirruccello, M., Milosevic, I., Gracheva, E.O., Bagriantsev, S.N., Borgese, N., and De Camilli, P. (2013). PI(4,5)P(2)-dependent and Ca(2+)-regulated ER-PM interactions mediated by the extended synaptotagmins. Cell *153*, 1494–1509.

Greenspan, P., Mayer, E.P., and Fowler, S.D. (1985). Nile red: a selective fluorescent stain for intracellular lipid droplets. J. Cell Biol. *100*, 965–973.

Hanada, K., Kumagai, K., Yasuda, S., Miura, Y., Kawano, M., Fukasawa, M., and Nishijima, M. (2003). Molecular machinery for non-vesicular trafficking of ceramide. Nature *426*, 803–809.

Harayama, T., and Riezman, H. (2018). Understanding the diversity of membrane lipid composition. Nat. Rev. Mol. Cell Biol. *19*, 281–296.

Holthuis, J.C., and Levine, T.P. (2005). Lipid traffic: floppy drives and a superhighway. Nat. Rev. Mol. Cell Biol. *6*, 209–220.

Holthuis, J.C., and Menon, A.K. (2014). Lipid landscapes and pipelines in membrane homeostasis. Nature *510*, 48–57.

Ito, M., Okino, N., and Tani, M. (2014). New insight into the structure, reaction mechanism, and biological functions of neutral ceramidase. Biochim. Biophys. Acta *1841*, 682–691.

Jain, A., and Holthuis, J.C.M. (2017). Membrane contact sites, ancient and central hubs of cellular lipid logistics. Biochim. Biophys. Acta Mol. Cell Res. *1864*, 1450–1458.

Kajiwara, K., Ikeda, A., Aguilera-Romero, A., Castillon, G.A., Kagiwada, S., Hanada, K., Riezman, H., Muñiz, M., and Funato, K. (2014). Osh proteins regulate COPII-mediated vesicular transport of ceramide from the endoplasmic reticulum in budding yeast. J. Cell Sci. *127*, 376–387.

Kajiwara, K., Watanabe, R., Pichler, H., Ihara, K., Murakami, S., Riezman, H., and Funato, K. (2008). Yeast *ARV1* is required for efficient delivery of an early GPI intermediate to the first mannosyltransferase during GPI assembly and controls lipid flow from the endoplasmic reticulum. Mol. Biol. Cell *19*, 2069–2082.

Kopec, K.O., Alva, V., and Lupas, A.N. (2010). Homology of SMP domains to the TULIP superfamily of lipid-binding proteins provides a structural basis for lipid exchange between ER and mitochondria. Bioinformatics *26*, 1927–1931.

Kurokawa, K., Okamoto, M., and Nakano, A. (2014). Contact of cis-Golgi with ER exit sites executes cargo capture and delivery from the ER. Nat. Commun. *5*, 3653.

Kus, G., Kabadere, S., Uyar, R., and Kutlu, H.M. (2015). Induction of apoptosis in prostate cancer cells by the novel ceramidase inhibitor ceranib-2. In Vitro Cell Dev. Biol. Anim. *51*, 1056–1063.

Levine, T.P., Wiggins, C.A., and Munro, S. (2000). Inositol phosphorylceramide synthase is located in the Golgi apparatus of *Saccharomyces cerevisiae*. Mol. Biol. Cell *11*, 2267–2281.

Liu, L.K., Choudhary, V., Toulmay, A., and Prinz, W.A. (2017). An inducible ER-Golgi tether facilitates ceramide transport to alleviate lipotoxicity. J. Cell Biol. *216*, 131–147.

Manford, A.G., Stefan, C.J., Yuan, H.L., Macgurn, J.A., and Emr, S.D. (2012). ER-to-plasma membrane tethering proteins regulate cell signaling and ER morphology. Dev. Cell *23*, 1129–1140.

Matsuura-Tokita, K., Takeuchi, M., Ichihara, A., Mikuriya, K., and Nakano, A. (2006). Live imaging of yeast Golgi cisternal maturation. Nature *441*, 1007–1010.

McNew, J.A., Coe, J.G., Søgaard, M., Zemelman, B.V., Wimmer, C., Hong, W., and Söllner, T.H. (1998). Gos1p, a *Saccharomyces cerevisiae* SNARE protein involved in Golgi transport. FEBS Lett. *435*, 89–95.

Melero, A., Chiaruttini, N., Karashima, T., Riezman, I., Funato, K., Barlowe, C., Riezman, H., and Roux, A. (2018). Lysophospholipids facilitate COPII vesicle formation. Curr. Biol. *28*, 1950–1958.

Min, S.W., Chang, W.P., and Südhof, T.C. (2007). E-Syts, a family of membranous Ca2+-sensor proteins with multiple C2 domains. Proc. Natl. Acad. Sci. U S A *104*, 3823–3828.

Nakazawa, N., Teruya, T., Sajiki, K., Kumada, K., Villar-Briones, A., Arakawa, O., Takada, J., Saitoh, S., and Yanagida, M. (2018). The putative ceramide-conjugation protein Cwh43 regulates G0 quiescence, nutrient metabolism and lipid homeostasis in fission yeast. J. Cell Sci. *131*, jcs217331.

Perry, R.J., and Ridgway, N.D. (2005). Molecular mechanisms and regulation of ceramide transport. Biochim. Biophys. Acta *1734*, 220–234.

Pittet, M., Uldry, D., Aebi, M., and Conzelmann, A. (2006). The N-glycosylation defect of cwh8Delta yeast cells causes a distinct defect in sphingolipid biosynthesis. Glycobiology *16*, 155–164.

Puoti, A., Desponds, C., and Conzelmann, A. (1991). Biosynthesis of mannosylinositolphosphoceramide in *Saccharomyces cerevisiae* is dependent on genes controlling the flow of secretory vesicles from the endoplasmic reticulum to the Golgi. J. Cell Biol. *113*, 515–525.

Quon, E., Sere, Y.Y., Chauhan, N., Johansen, J., Sullivan, D.P., Dittman, J.S., Rice, W.J., Chan, R.B., Di Paolo, G., Beh, C.T., and Menon, A.K. (2018). Endoplasmic reticulum-plasma membrane contact sites integrate sterol and phospholipid regulation. PLoS Biol. *16*, e2003864.

Radulovic, M., Knittelfelder, O., Cristobal-Sarramian, A., Kolb, D., Wolinski, H., and Kohlwein, S.D. (2013). The emergence of lipid droplets in yeast: current status and experimental approaches. Curr. Genet. *59*, 231–242.

Schauder, C.M., Wu, X., Saheki, Y., Narayanaswamy, P., Torta, F., Wenk, M.R., De Camilli, P., and Reinisch, K.M. (2014). Structure of a lipid-bound extended synaptotagmin indicates a role in lipid transfer. Nature *510*, 552–555.

Schulz, T.A., and Creutz, C.E. (2004). The tricalbin C2 domains: lipid-binding properties of a novel, synaptotagmin-like yeast protein family. Biochemistry *43*, 3987–3995.

Senkal, C.E., Salama, M.F., Snider, A.J., Allopenna, J.J., Rana, N.A., Koller, A., Hannun, Y.A., and Obeid, L.M. (2017). Ceramide is metabolized to acylceramide and stored in lipid droplets. Cell Metab. *25*, 686–697.

Sezgin, E., Levental, I., Mayor, S., and Eggeling, C. (2017). The mystery of membrane organization: composition, regulation and roles of lipid rafts. Nat. Rev. Mol. Cell Biol. *18*, 361–374.

Simons, K., and Ikonen, E. (1997). Functional rafts in cell membranes. Nature *387*, 569–572.

Tani, M., and Funato, K. (2018). Protection mechanisms against aberrant metabolism of sphingolipids in budding yeast. Curr. Genet. *64*, 1021–1028.

Tarassov, K., Messier, V., Landry, C.R., Radinovic, S., Serna Molina, M.M., Shames, I., Malitskaya, Y., Vogel, J., Bussey, H., and Michnick, S.W. (2008). An *in vivo* map of the yeast protein interactome. Science *320*, 1465–1470.

Toulmay, A., and Prinz, W.A. (2012). A conserved membrane-binding domain targets proteins to organelle contact sites. J. Cell Sci. *125*, 49–58.

Umemura, M., Fujita, M., Yoko-O, T., Fukamizu, A., and Jigami, Y. (2007). *Saccharomyces cerevisiae CWH43* is involved in the remodeling of the lipid moiety of GPI anchors to ceramides. Mol. Biol. Cell *18*, 4304–4316.

van Meer, G., Voelker, D.R., and Feigenson, G.W. (2008). Membrane lipids: where they are and how they behave. Nat. Rev. Mol. Cell Biol. *9*, 112–124.

Voynova, N.S., Roubaty, C., Vazquez, H.M., Mallela, S.K., Ejsing, C.S., and Conzelmann, A. (2015). *Saccharomyces cerevisiae* is dependent on vesicular traffic between the Golgi apparatus and the vacuole hhen inositolphosphorylceramide synthase Aur1 is inactivated. Eukaryot. Cell *14*, 1203–1216.

Voynova, N.S., Vionnet, C., Ejsing, C.S., and Conzelmann, A. (2012). A novel pathway of ceramide metabolism in *Saccharomyces cerevisiae*. Biochem. J. *447*, 103–114.

Walther, T.C., and Farese, R.V., Jr. (2012). Lipid droplets and cellular lipid metabolism. Annu. Rev. Biochem. *81*, 687–714.

Yabuki, Y., Ikeda, A., Araki, M., Kajiwara, K., Mizuta, K., and Funato, K. (2019). Sphingolipid/Pkh1/2-TORC1/Sch9 signaling regulates ribosome biogenesis in tunicamycin-induced stress response in yeast. Genetics *212*, 175–186.

Yamaji, T., and Hanada, K. (2015). Sphingolipid metabolism and interorganellar transport: localization of sphingolipid enzymes and lipid transfer proteins. Traffic *16*, 101–122.

Yu, H., Liu, Y., Gulbranson, D.R., Paine, A., Rathore, S.S., and Shen, J. (2016). Extended synaptotagmins are Ca2+-dependent lipid transfer proteins at membrane contact sites. Proc. Natl. Acad. Sci. U S A *113*, 4362–4367.

iScience, Volume *23*

Supplemental Information

Tricalbins Are Required for Non-vesicular Ceramide Transport at ER-Golgi Contacts and Modulate Lipid Droplet Biogenesis

Atsuko Ikeda, Philipp Schlarmann, Kazuo Kurokawa, Akihiko Nakano, Howard Riezman, and Kouichi Funato

SUPPLEMENTAL FIGURES

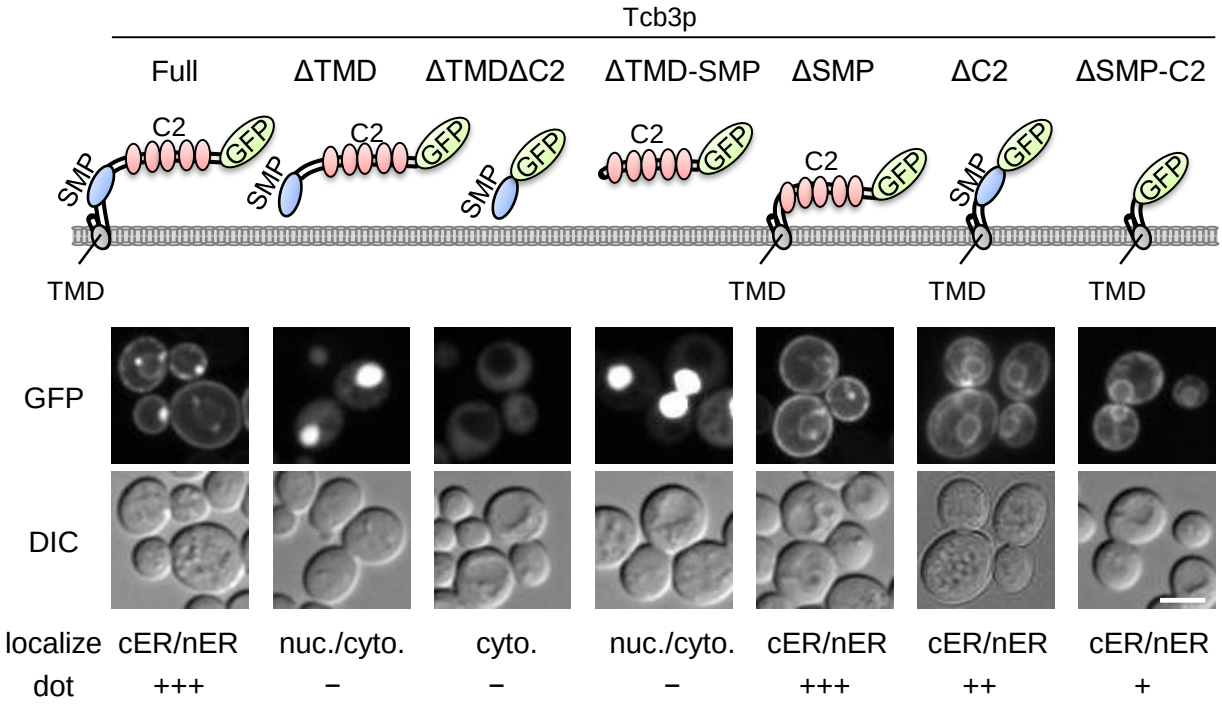

Figure S1. Truncated forms of Tcb3 lacking the transmembrane domain are distributed in the cytosol or nucleus, Related to Figure 1

*tcb3*Δ cells overexpressing Tcb3-GFP, Tcb3(ΔTMD)-GFP, Tcb3(ΔTMDΔC2)-GFP, Tcb3(ΔTMD-SMP)-GFP, Tcb3(ΔSMP)-GFP, Tcb3(ΔC2)-GFP or Tcb3(ΔSMP-C2)-GFP under *TDH3* promoter were grown at 25˚C and imaged by DIC and fluorescence microscopy. Scale bar, 5 μm.

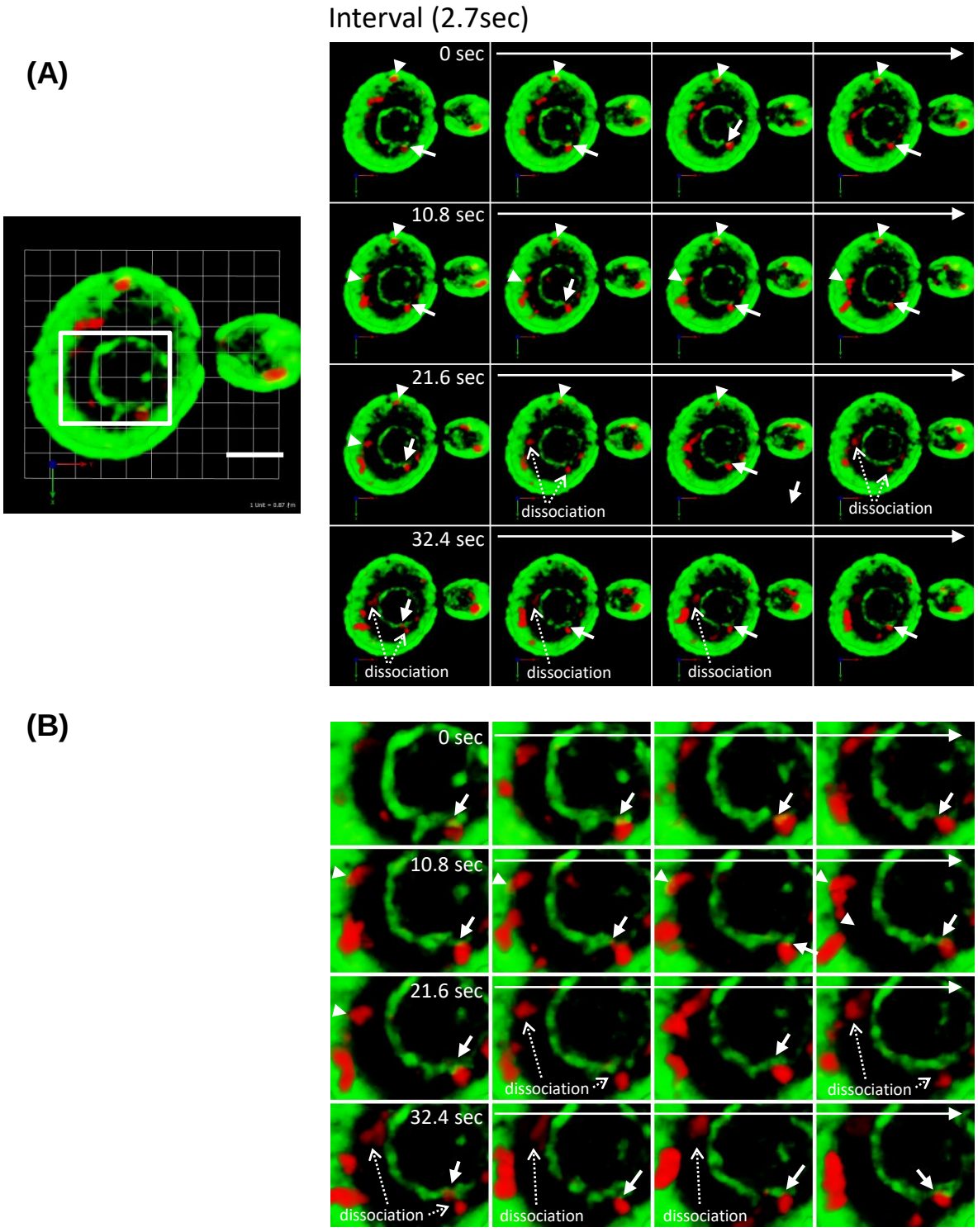

Figure S2. **Dynamic behaviors of ER-medial-Golgi contact sites, Related to Figure 2**

(A, B) *tcb3*Δ cells expressing Tcb3-GFP with mRFP-Gos1 under *TDH3* promoter were observed with SCLIM as in Fig 2B. Representative 3D images of a whole cell are shown. Right panels show time-lapse images (A). The boxed areas of the images in (A) are shown in an enlarged view (B). Scale bar, 2 μm. Arrows in the images indicate nER-medial-Golgi contact sites and arrowheads point to cER-medial-Golgi contact sites. The medial-Golgi contacts the nER or the cER (arrows and arrowheads) and then leave (dashed arrows).

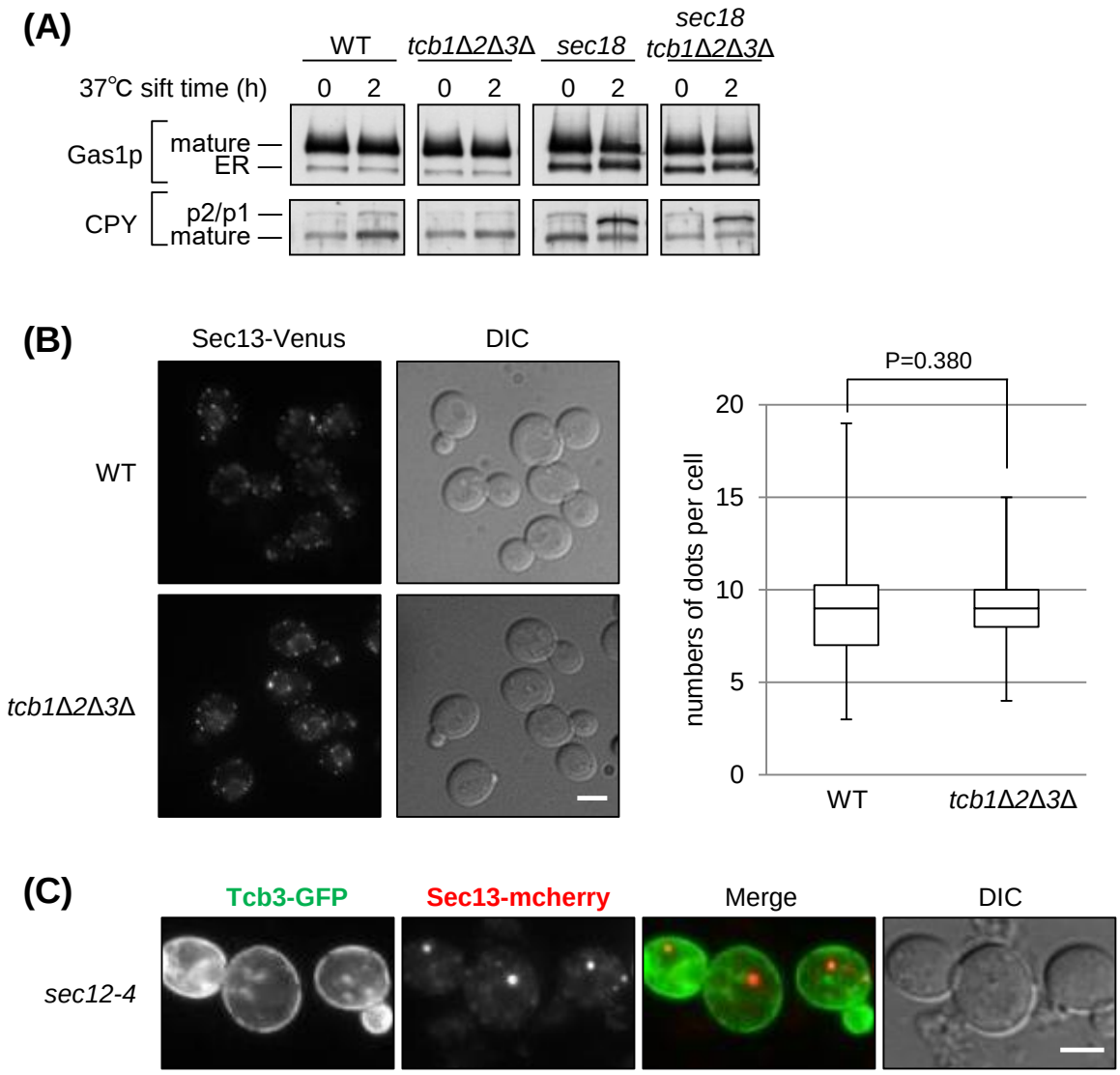

Figure S3. Tcb proteins are not required for ER-to-Golgi vesicular transport of proteins, Related to Figure 2 and Figure 4

(A) Cells were grown at 25˚C, shifted to 37˚C for 2 h. Cell lysates were prepared, subjected to SDS-PAGE, and analyzed by western blotting using antibodies against Gas1p and CPY. mature, mature forms of Gas1p and CPY; ER, immature ER form of Gas1p; p1 and p2, ER and Golgi forms of CPY, respectively.
(B) Cells expressing Sec13-Venus were grown at 25 ˚C and imaged by DIC and fluorescence microscopy. Scale bar, 5 μm. Numbers of dots per cell were counted. The box plot of the number of dots from more than 100 cells for each strain was shown. P value by Student's t-test.
(C) *sec12-4* cells expressing Tcb3-GFP and Sec13-mCherry were grown at 25˚C, sifted to 30˚C for 1 h, and imaged by DIC and fluorescence microscopy. Scale bar, 5 μm.

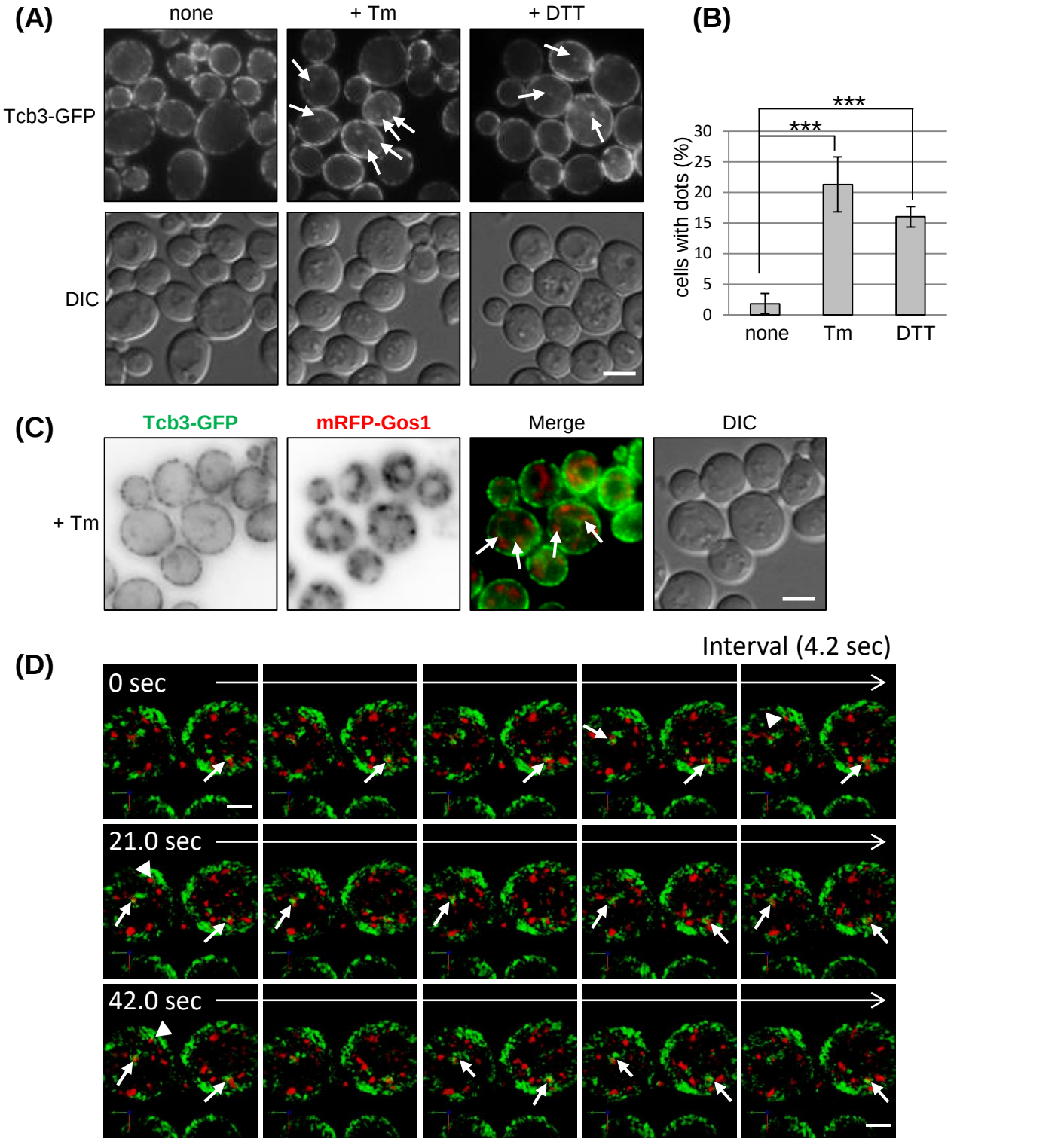

Figure S4. Tcb3p moves to nER-Golgi contact site in response to ER stress, Related to Discussion

(A, B) Cells expressing Tcb3p tagged with GFP at the C terminus under the control of *TCB3* endogenous promoter were grown at 25˚C, treated without and with tunicamycin (2.5 μg/ml, 4 h) or DTT (10 mM, 4 h), and imaged by differential interference contrast (DIC) and fluorescence microscopy. Arrows in the images indicate Tcb3-GFP dots (A). Scale bar, 5 μm. Percentages of cells with GFP dots were quantified, and the data represent the mean ± SD of three independent experiments; n > 300 cells. *** $P < 0.001$ by Student's t-test. (B).

(C, D) The same cells as in (A) were transformed with mRFP-*GOS1* plasmid, treated with tunicamycin (2.5 μg/ml, 4 h), and imaged by DIC and fluorescence microscopy (scale bar, 5 μm) (C). Cells were also observed with SCLIM (scale bar, 2 μm) (D). Arrows in the images indicate nER-medial-Golgi contact sites and arrowheads point to cER-medial-Golgi contact sites.

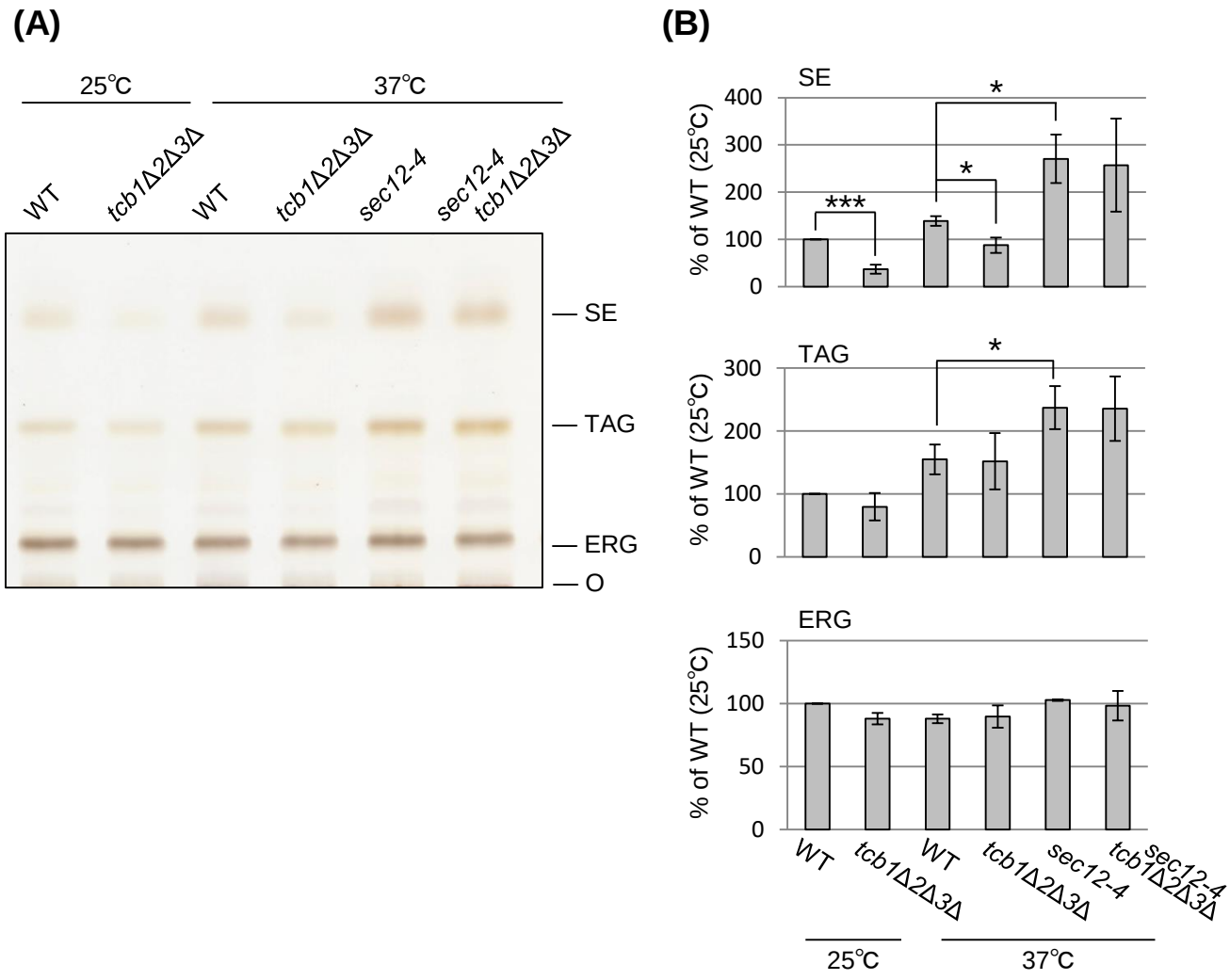

Figure S5. TLC analysis of the neutral lipids, Related to Discussion

Total lipids were extracted from wild-type and mutant cells grown at 25˚C or sifted to 37˚C for 30 minutes and separated on TLC plates (A). The positions of sterol ester (SE), triacylglycerol (TAG), ergosterol (ERG) and origin (O) are indicated. The bands were quantified with ImageJ and the relative levels of lipids to wild type cells grown at 25˚C were presented as percentage (B). Data represent mean ± SD of three independent experiments. *, $P < 0.05$; ***, $P < 0.001$ by Student's t-test.

SUPPLEMENTAL TABLES

Table S1. - Plasmids used in this study, Related to All Figures

Plasmid	Relevant information	Sorce
pRS416-*TDH3*/*TCB3*-GFP	*CEN,* yeast *TDH3* promoter, *TCB3-GFP*, *URA3*	This study
pRS416-*TDH3*/*TCB3*(ΔC2-SMP)-GFP	*CEN,* yeast *TDH3* promoter, $TCB3^{1F\text{-}259R}$*-GFP*, *URA3*	This study
pRS416-*TDH3*/*TCB3*(ΔSMP)-GFP	*CEN,* yeast *TDH3* promoter, $TCB3^{260F\text{-}488R\Delta}$*-GFP*, *URA3*	This study
pRS416-*TDH3*/*TCB3*(ΔC2)-GFP	*CEN,* yeast *TDH3* promoter, $TCB3^{1F\text{-}489R}$*-GFP*, *URA3*	This study
pRS416-*TDH3*/*TCB3*(ΔTMD)-GFP	*CEN,* yeast *TDH3* promoter, $TCB3^{260F\text{-}1546R}$*-GFP*, *URA3*	This study
pRS416-*TDH3*/*TCB3*(ΔTMD-SMP)-GFP	*CEN,* yeast *TDH3* promoter, $TCB3^{490F\text{-}1546R}$*-GFP*, *URA3*	This study
pRS416-*TDH3*/*TCB3*(ΔTMD ΔC2)-GFP	*CEN,* yeast *TDH3* promoter, $TCB3^{260F\text{-}489R}$*-GFP*, *URA3*	This study
pRS314-*TDH3*/ mRFP-*SED5*	*CEN*, yeast *TDH3* promoter, *mRFP-SED5*, *TRP1*	Provided by A. Nakano (Matsuura-Tokita et al., 2006)
pRS314-*TDH3*/ mRFP-*GOS1*	*CEN*, yeast *TDH3* promoter, *mRFP-GOS1*, *TRP1*	Provided by A. Nakano

		(Matsuura-Tokita et al., 2006)
YCplac22 / *SEC7*-mRFP	*CEN*, yeast *ADH1* promoter, *SEC7-mRFP*, *TRP1*	This study
pRS413-*ADH1* / *Kar2-SS-GFP-HDEL*	*CEN, yeast ADH1* promoter, *KAR2(1-135)-GFP-HDEL, HIS3*	This study
pRS416-*TDH3*	*CEN*, yeast *TDH3* promoter, *URA3*	Provided by M. Funk (Mumberg et al., 1995)
pRS413-*ADH1*	*CEN*, yeast *ADH1* promoter, *HIS3*	Provided by M. Funk (Mumberg et al., 1995)
pRS416-*TDH3* / *TCB3*	*CEN*, yeast *TDH3* promoter, *TCB3, URA3*	This study
pRS416-*TDH3* / *TCB3*(ΔC2-SMP)	*CEN,* yeast *TDH3* promoter, $TCB3^{1F\text{-}259R}$, *URA3*	This study
pRS416-*TDH3* / *TCB3*(ΔSMP)	*CEN,* yeast *TDH3* promoter, $TCB3^{260F\text{-}488R\Delta}$, *URA3*	This study
pRS416-*TDH3* / *TCB3*(ΔC2)	*CEN,* yeast *TDH3* promoter, $TCB3^{1F\text{-}489R}$, *URA3*	This study

Table S2 - Yeast strains used in this study, Related to All Figures

Strain	Genotype	Sorce
FKY66 / RH5574	MAT**alpha** *ura3 leu2 his3 trp1 bar1*	This study
FKY73 / RH5578	MAT**alpha** *ura3 leu2 his3 trp1 lys2 bar1 tcb1Δ::TRP1 tcb2Δ::HIS3 tcb3Δ::LEU2*	This study
FKY74 / RH5579	MAT**alpha** *ura3 leu2 his3 trp1 bar1 sec18-20*(ts)	This study
FKY76 / RH5584	MAT**alpha** *ura3 leu2 his3 trp1 lys2 bar1 sec18-20*(ts) *tcb1Δ::TRP1 tcb2Δ::HIS3 tcb3Δ::LEU2*	This study
FKY2924	MAT**a** *ura3 leu2 his3 trp1 lys2 bar1 tcb3Δ::LEU2*	This study
FKY2926	MAT**a** *ura3 leu2 his3 trp1 bar1 sec18-20*(ts) *tcb1Δ::TRP1 tcb2Δ::HIS3 tcb3Δ::LEU2*	This study
FKY2927	MAT**a** *ura3 leu2 his3 trp1 lys2 bar1 tcb1Δ::TRP1 tcb2Δ::HIS3 tcb3Δ::LEU2*	This study
FKY2928	MAT**alpha** *ura3 leu2 his3 trp1 lys2 bar1*	This study
FKY2929	MAT**alpha** *ura3 leu2 his3 trp1 bar1 sec18-20*(ts)	This study
FKY2960	MAT**a** *usa3 leu2 his3 lys2 bar1 sec12-4*(ts)	This study
FKY2984	MAT**alpha** *ura3 leu2 his3 trp1 lys2 bar1 sec12-4*(ts) *tcb1Δ::TRP1 tcb2Δ::HIS3 tcb3Δ::LEU2*	This study

FKY3343	MAT**a** *ura3 leu2 his3 trp1 lys2 bar1 TCB3-GFP::TRP1*	This study
FKY4663	MAT**a** *ura3 leu2 his3 trp1 lys2 bar1 SEC13-Venus::KanMX*	This study
FKY4876	MAT**a** *ura3 leu2 his3 trp1 lys2 bar1 tcb1Δ::TRP1 tcb2Δ::HIS3 tcb3Δ::LEU2 SEC13-Venus::KanMX*	This study
FKY4892	MAT **alpha** *ura3 leu2 his3 trp1 lys2 ade2 dga1Δ:: KanMX lro1Δ:: KanMX*	This study
FKY4987	MAT**a** *ura3 leu2 his3 lys2 bar1 sec12-4*(ts) *tcb3Δ::LEU2 SEC13-mCherry::KanMX*	This study
FKY5167	MAT **alpha** *ura3 leu2 his3 trp1 lys2 bar1 tcb1Δ::KanMX tcb2Δ::HIS3 tcb3Δ::LEU2*	This study

TRANSPARENT METHODS

Strains and Plasmids

All yeast plasmids and strains used in this study are listed in Table S1 and S2, respectively. Yeast cultivations, genetic manipulation and strain construction were carried out as described previously (Kajiwara et al., 2015, 2008). GFP-, Venus- and mCherry-tagged strains and *tcb* deletion strains were generated by PCR based one step gene replacement. Then, *tcb1*Δ*2*Δ*3*Δ strain was crossed with *sec18-20* or *sec12-4* strain to obtain the *sec tcb* combined double, triple and quadruple mutant strains. To construct the Tcb3-GFP, Tcb3(ΔSMP-C2)-GFP, Tcb3(ΔSMP)-GFP, Tcb3(ΔC2)-GFP and Tcb3p overexpression plasmids (*TCB3*, *TCB3*-ΔSMP, *TCB3*-ΔC2 and *TCB3*-ΔSMP-C2), appropriate regions of *TCB3* which were PCR amplified from yeast genomic DNA and GFP regions which obtained from pGREG600, were inserted into pRS416-*TDH3*. YCplac22/*SEC7*-mRFP plasmid was constructed from YCplac22 and pRS316-ADH/*SEC7*-Mrfp (Kurokawa et al., 2014). The BamHI-ClaI fragment containing Kar2p signal-peptide sequence (1-135) and the ClaI-XhoI fragment containing TAT2-mRFP were cloned into the BamHI-XhoI site of pRS413-ADH to generate pRS413-ADH/Kar2-SS-GFP-HDEL.

Fluorescence microscopy

Cells were grown overnight in SD medium including the appropriate nutrients to select for plasmids, and imaged by differential interference contrast (DIC) and fluorescence microscopy. GFP signals were measured by the Image J software. For parallel section observation, images were taken at z-sections with 0.2 μm parallel

intervals. For lipid droplet detection, cells were treated with Nile Red (final concentration to be 1μg/ml) for 10 minutes, and imaged by fluorescence microscopy. Fluorescence observation by super-resolution confocal live imaging microscopy (SCLIM) was performed as described previously (Kurokawa et al., 2014).

Lipid labelling

In vivo labelling of lipids with [^{3}H]*myo*-inositol (Perkin Elmer, Inc.) or [^{3}H]dihydrosphingosine (DHS; American Radiolabeled Chemicals Inc.) was performed as described previously (Kajiwara et al., 2008). Radiolabeled lipids were extracted with chloroform-methanol-water (10:10:3, vol/vol/vol), and analyzed by thin-layer chromatography (TLC) using solvent system I, chloroform-methanol-0.25% KCl (55:45:10, vol/vol/vol) for complex sphingolipid labeled with [^{3}H]*myo*-inositol and solvent system II, chloroform-methanol-4.2 N ammonium hydroxide (9:7:2, vol/vol/vol) for sphingolipid labeled with [^{3}H]DHS. For ceramide and acylceramide analysis, the lipids labelled with [^{3}H]DHS were first separated on TLC plates as above. Subsequently, fractions containing ceramides and actlceramides, which are approximately 2–3 cm from the top of the TLC plates (Kajiwara et al., 2012), were collected by scraping and eluting with chloroform-methanol (1:1, v/v), and analyzed by TLC using solvent system III, chloroform-methanol-2M ammonium hydroxide (40:10:1, vol/vol//vol) (Voynova et al., 2012). Radiolabeled sphingolipids were visualized and quantified on an FLA-7000 system.

Western blot analysis

Preparation of cell lysates and western blot analysis were performed as described

previously (Kajiwara et al., 2008). Blots were probed with rabbit polyclonal antibodies against Gas1p and CPY and a peroxidase-conjugated affinity-purified anti-rabbit IgG antibody.

Neutral lipid analysis

For the analysis of neutral lipids, cells corresponding to 10 OD_{600} were disrupted with glass beads, and lipids were extracted with chloroform-methanol-water (10:10:3, vol/vol/vol). The lipid extracts were applied to two step TLC as described before (Athenstaedt et al., 1999; Froissard et al., 2015); first step using petroleum-diethyl ether-acetic acid (25:25:1, vol/vol/vol) for the first third of the total distance and second step using petroleum-diethyl ether (49:1, vol/vol). To visualize the separated bands of neutral lipids, the TLC plates were dipped for 10 s into a developing solution (0.63 g of $MnCl_2 \cdot 4H_2O$, 60 ml of water, 60 ml of methanol, and 4 ml of concentrated sulfuric acid), briefly dried, and heated at 100°C for 30 min. Quantification of lipids was carried out using ImageJ.

SUPPLEMENTAL REFERENCES

Athenstaedt, K., Zweytick, D., Jandrositz, A., Kohlwein, S.D., and Daum, G. (1999) Identification and characterization of major lipid particle proteins of the yeast *Saccharomyces cerevisiae*. *J Bacteriol* 181, 6441-6448.

Froissard, M., Canonge, M., Pouteaux, M., Cintrat, B., Mohand-Oumoussa, S., Guillouet, S.E., Chardot, T., Jacques, N., and Casaregola, S. (2015) Lipids containing medium-chain fatty acids are specific to post-whole genome duplication *Saccharomycotina* yeasts. *BMC Evol Biol* 15, 97.

Kajiwara, K., Ikeda, A., Aguilera-Romero, A., Castillon, G.A., Kagiwada, S., Hanada, K., Riezman, H., Muñiz, M., and Funato, K. (2014). Osh proteins regulate COPII-mediated vesicular transport of ceramide from the endoplasmic reticulum in budding yeast. *J Cell Sci* 127, 376-387.

Kajiwara, K., Muneoka, T., Watanabe, Y., Karashima, T., Kitagaki, H., Funato, K. (2012). Perturbation of sphingolipid metabolism induces endoplasmic reticulum stress-mediated mitochondrial apoptosis in budding yeast. *Mol Microbiol* 86, 1246-1261.

Kajiwara, K., Watanabe, R., Pichler, H., Ihara, K., Murakami, S., Riezman, H., and Funato, K. (2008). Yeast ARV1 is required for efficient delivery of an early GPI intermediate to the first mannosyltransferase during GPI assembly and controls lipid flow from the endoplasmic reticulum. *Mol Biol Cell* 19, 2069-2082.

Kurokawa, K., Okamoto, M., and Nakano, A. (2014). Contact of cis-Golgi with ER exit sites executes cargo capture and delivery from the ER. *Nat Commun* 5, 3653.

Matsuura-Tokita, K., Takeuchi, M, Ichihara, A., Mikuriya, K., and Nakano, A. (2006). Live imaging of yeast Golgi cisternal maturation. *Nature* 441, 1007-1010.

Mumberg, D., Müller, R., and Funk, M. (1995). Yeast vectors for the controlled expression of heterologous proteins in different genetic backgrounds. *Gene* 156, 119-122.

Voynova, N.S., Vionnet, C., Ejsing, C.S., and Conzelmann, A. (2012). A novel pathway of ceramide metabolism in Saccharomyces cerevisiae. *Biochem J* 447, 103-114.